

# 1

## Introduction

**Abstract:** This chapter presents a brief introduction of micropositioning systems and their concerned design and control problems. The compliant translational and rotational guiding mechanisms are described, the related actuation and sensing issues are raised, and the motion control problem is summarized. An outline of the remaining chapters of the book is provided.

**Keywords:** Micropositioning, Compliant mechanisms, Flexure hinges, Translational guiding, Rotational guiding, Actuators, Sensors, Control.

### 1.1 Micropositioning Techniques

Micropositioning systems refer to precision positioning devices which are capable of delivering displacement down to sub-micrometer resolution and accuracy. Micropositioning devices have been widely applied in the domain of precision manipulation and manufacturing, such as scanning probe microscopy, lithography manufacturing, and wafer alignment. To cater for the precision demands in relatively low-loading applications, flexure-based compliant mechanisms have been widely employed. Unlike traditional mechanical joints, the repeatable output motion of a flexible element is generated by the elastic deformation of the material. As a consequence, compliant mechanisms enable some attractive advantages – including no backlash, no friction, no wear, low cost, vacuum compatibility, etc. [1, 2].

According to the motion property, micropositioning can be classified into two general categories in terms of translational and rotational micropositioning. The combination of these two types of motion forms a hybrid micropositioning. Typical flexure mechanisms can deliver a translational displacement of less than 1 mm and a rotational displacement smaller than  $1^\circ$  within the yield strength of the materials. In modern precision engineering applications, there is a growing demand for micropositioning systems which are capable of producing large-range (e.g., over 10 mm or  $10^\circ$ ) precision motion, yet have a compact size at the same time. Such applications involve large-range scanning probe microscopy [3], lithography and fabrication [4], biological micromanipulation [5], etc. For instance, in automated zebrafish embryo manipulation, a precise positioning stage with a long stroke is needed to execute accurate operation [6].

In addition, a precision positioning stage with compact size allows the application inside a constrained space. For example, a compact positioning device is required to provide ultrahigh-precision positioning of the specimens and tools inside the chamber of scanning electron microscopes for automated probing and micromanipulation [7]. Moreover, a compact physical size enables cost reduction in terms of material and fabrication. Hence, this book is concentrated on the design and implementation of compact micropositioning stages with large motion ranges.

## 1.2 Compliant Guiding Mechanisms

Concerning the motion guiding mechanism of the positioning stage, although aerostatic bearings [8] and maglev bearings [9] are usually adopted, flexure bearings are more attractive in the recent development of micropositioning systems, due to the aforementioned merits of compliant mechanisms [10]. Compared with other mechanisms, compliant flexures can generate a smooth motion by making use of the elastic deformation of the material. Nevertheless, their motion range is constricted by the yield strength of the material, which poses a great challenge to achieving a long stroke. From this point of view, once the kinematic scheme is determined, the structural parameters of the flexure mechanism call for a careful design to make sure that the material operates in the elastic domain without plastic deformation and fatigue failure.

Given the requirements on the motion or force property, a compliant guiding mechanism can be designed by resorting to different approaches, such as the rigid-body replacement method [11], building-block method [12], topology optimization method [13], topology synthesis method [14], etc. Without loss of generality, the element flexure hinges and the translational and rotational positioning mechanisms are introduced in the following sections.

### 1.2.1 Basic Flexure Hinges

A basic flexure hinge functions as a revolute joint. In the literature, various profiles of flexure hinges have been used to construct a flexure stage [15]. For example, the in-plane profiles of typical flexure hinges including right-circular, elliptic, right-angle, corner-filled, and leaf hinges are shown in Fig. 1.1. More types of flexure hinges are referred to in the books [2, 16].

Referring to Fig. 1.1, if one terminal  $A$  of the flexure hinge is fixed and the other terminal  $B$  has an applied force  $F_x$  along the  $x$ -axis or a moment  $M_z$  around the  $z$ -axis, an in-plane bending deformation of the hinge will be induced. Generally, these element flexure hinges are considered as revolute joints, which deliver a rotational motion of the terminal  $B$  with respect to the fixed terminal  $A$  around a rotation center. To generate a translational motion or a multi-axis rotational motion like a universal or spherical joint, multiple basic flexure hinges can be combined to construct a compound flexure hinge [17].

During the bending deformation of the element flexure hinge, the rotation center will be varied. The notch-type flexure hinge, especially the right-circular hinge, is able to deliver a rotation with smaller amount of center shift. However, this is achieved at the cost of a relatively small rotational motion range due to the stress concentration effect. In order to accomplish a large motion range, the leaf flexure hinge is usually employed due to the mitigation of the stress concentration effect. In addition, leaf flexures have been widely employed in micromechanism

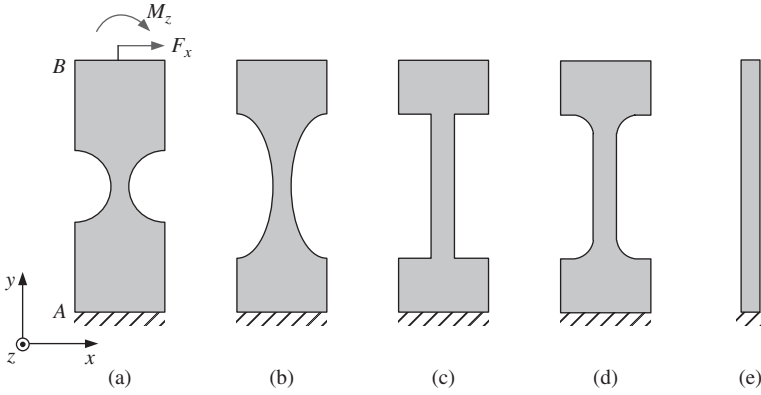


**Figure 1.1** Profiles of typical flexure hinges: (a) right-circular hinge; (b) elliptic hinge; (c) right-angle hinge; (d) corner-filled hinge; (e) leaf hinge.

design in microelectromechanical systems (MEMS) devices [18]. The design methods of the beam-based leaf flexures are referred to in the book [1].

### 1.2.2 Translational Flexure Hinges

As a compound type of flexure, parallelogram flexure is a popular design to achieve translational motion. For example, the translational flexure hinges constructed by right-circular hinges are shown in Fig. 1.2. To generate a larger translational motion range, the translational flexure hinges can be designed using leaf hinges, as shown in Fig. 1.3.

As shown in Fig. 1.3(a), when the output stage of a parallelogram flexure translates a displacement  $d_x$  in the  $x$ -axis, it also undergoes a parasitic translation  $d_y$  in the  $y$ -axis. For some applications, the translation  $d_y$  can be employed to enhance the resolution of the displacement due to the displacement deamplification effect. Concerning a large-range positioning in the

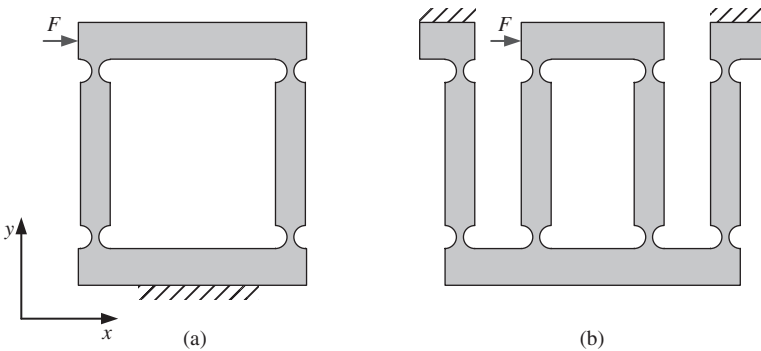


**Figure 1.2** Translational flexure hinges constructed by right-circular hinges: (a) parallelogram flexure; (b) compound parallelogram flexure (CPF).

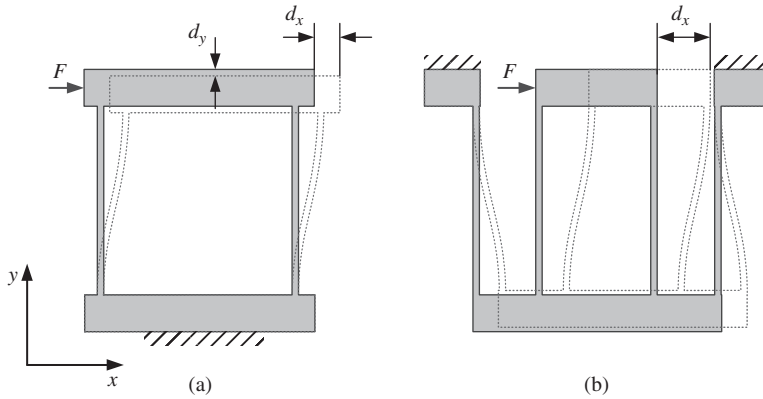


**Figure 1.3** Translational flexure hinges constructed by leaf hinges: (a) parallelogram flexure; (b) compound parallelogram flexure (CPF).

specified direction, the parasitic translation  $d_y$  is unwanted. In order to obtain a larger straight motion while eliminating the parasitic translation, a compound parallelogram flexure (CPF), as shown in Fig. 1.3(b), can be employed.

Intuitively, a longer stroke can be realized by using a longer and more slender leaf flexure. However, in practice, the length of the flexure hinge is constrained by the requirement of compactness and the minimum width is restricted by the tolerance of the manufacturing process. It is challenging to design a flexure micropositioning stage with a large stroke and compact size simultaneously. To overcome the aforementioned problem, the concept of multi-stage compound parallelogram flexure (MCPF) [19], as shown in Fig. 1.4(a), is employed in this book.

Compared with conventional CPF, the motion range of a MCPF is enlarged  $N$  times without changing the length and width of the flexures, where  $N$  is the number of basic CPF modules. Note that CPF is a special case of MCPF with  $N = 1$ . To enhance the transverse stiffness in the  $y$ -axis direction, an improved MCPF is presented as shown in Fig. 1.4(b), which is constructed by connecting the two secondary stages together.

### 1.2.3 Translational Positioning Mechanisms

A translational positioning mechanism is usually required to provide the translational motion in the two-dimensional plane or three-dimensional space. To generate the translational positioning in more than one direction, a suitable mechanism design is necessary. As far as a kinematic scheme is concerned, the positioning stages, which are capable of multi-dimensional translations, can be classified into two categories in terms of serial and parallel kinematics. The majority of the commercially available stages employ a serial-kinematic scheme. For example, some micropositioning stages have been developed by stacking the second single-axis positioning stage on top of the first one or nesting the second stage inside the first one [20–22]. In this way, the entire second stage is carried by the first one, as illustrated in Fig. 1.5(a), where the X stage serves as the output platform of the XY stage. As an example, the computer-aided design (CAD) model of a serial-kinematic XY stage is shown in Fig. 1.6(a), where the parallelogram flexures are constructed using right-circular hinges.

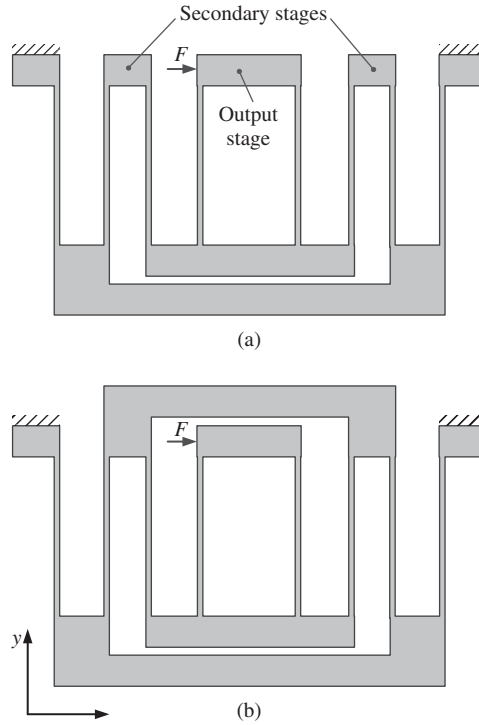


**Figure 1.4** (a) A multi-stage compound parallelogram flexure (MCPF) with two modules; (b) an improved MCPF with enhanced transverse stiffness in the  $y$ -axis.

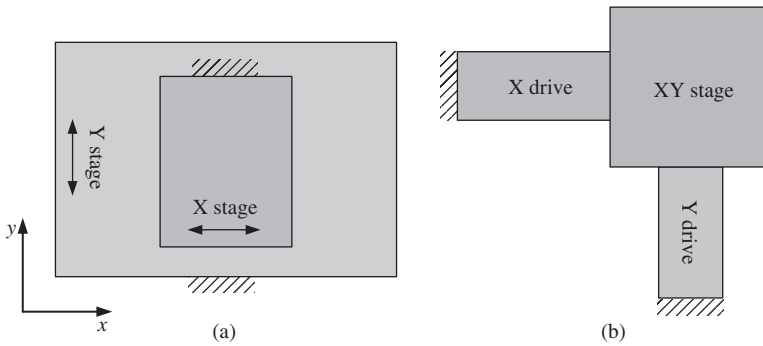


**Figure 1.5** Illustrations of (a) serial-kinematic XY stage and (b) parallel-kinematic XY stage.

Even though a compact structure may be achieved by using the serial-kinematic design [22], it is at the cost of high inertia, low resonant frequency, and large cumulative errors. A further disadvantage is that the dynamic characteristics in the different working axes are usually unequal for a serial-kinematic stage. On the contrary, a parallel-kinematic scheme [23, 24]

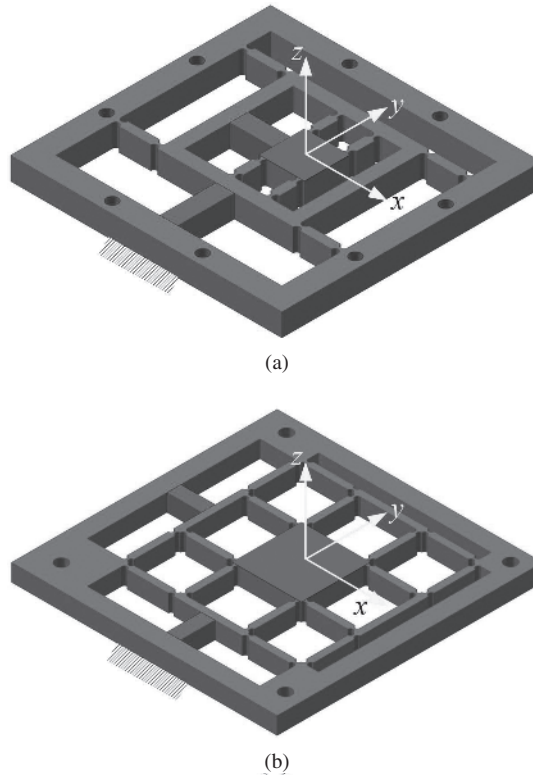


**Figure 1.6** Examples of (a) serial-kinematic XY compliant stage and (b) parallel-kinematic XY compliant stage.

overcomes the aforementioned disadvantages. Different from serial-kinematic mechanisms, the end-effector of a parallel-kinematic mechanism is carried by multiple kinematic linkages in a closed-loop manner [25]. As illustrated in Fig. 1.5(b), the output platform is driven by X and Y drives in parallel. Unlike the serial-kinematic design, it allows the achievement of low inertia, high resonant frequency, no cumulative error, high load capacity, and identical dynamic features in the different working axes. Thus, the flexure-based parallel-kinematic compliant mechanisms pave a promising way to achieve ultrahigh-precision positioning. For instance, the CAD model of a parallel-kinematic XY stage is shown in Fig. 1.6(b). Although the right-circular hinges are adopted as examples to construct the parallelogram flexures, any other types of hinges (e.g., leaf flexures) can also be employed to design the XY stage.

To facilitate the control design for the micropositioning systems, the micropositioning stages are desirable to provide a decoupled output motion. Output decoupling means that the output motion in one working axis does not induce motion in the other axes of the stage. Additionally, input decoupling indicates that the actuation provided by one motor does not cause a force or load on the other motors of the stage. The purpose of input decoupling is to isolate and protect the actuators for a micropositioning system. A total decoupling stage possesses the

properties of both output decoupling and input decoupling. The XY stage shown in Fig. 1.6(b) is desired to possess total decoupling characteristics. However, such a standard flexure-based XY micropositioning stage is restricted to deliver a small translational range, partially because of the stress stiffening effect.

Stress stiffening is a geometrical nonlinearity. It is most pronounced in structures which are thin in one or more dimensions. Given a structure based on flexure hinges as shown in Fig. 1.1, the stress stiffening indicates that the lateral stiffness in the  $x$ -axis of the structure can be significantly increased (or decreased) by the tensile (or compressive) axial stress in the  $y$ -axis of the structure. Generally, this phenomenon should be avoided because it increases the actuation force requirement and reduces the stroke of the motor, and causes nonlinearities in actuation. This book presents the design of large-range micropositioning systems with the stress stiffening effect mitigated greatly.

Recently, some compliant XY stages have been proposed to deliver a large motion range over 1 mm [26–29]. However, the developed stages have a relatively large dimension. As a result, the stages possess a small area ratio, which is defined as the ratio between the area of the planar workspace and the area of the planar dimension of the XY stage. To achieve a large motion range while keeping a compact structure, the MCPFs are proposed to devise new compliant parallel-kinematic XY stages in this book.

In addition, as a spatial mechanism, a traditional XYZ micropositioning stage is shown in Fig. 1.7. This XYZ stage is called a three-prismatic-universal-universal (3-PUU) parallel mechanism [30]. The cube-like output platform is supported by three identical limbs, which are arranged orthogonally and connected in parallel. Each limb consists of a serial connection of one prismatic (P) hinge and two universal (U) hinges. Each universal hinge includes two orthogonally arranged notch-type revolute (R) hinges. The XYZ stage delivers a nearly decoupled output translation in the three-dimensional space. However, the motion range is limited due to the relatively small rotational angle of the notch-type flexure hinges.

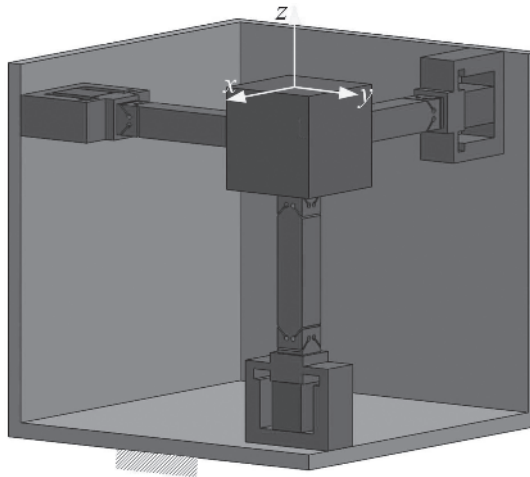


**Figure 1.7** Example of a parallel-kinematic XYZ compliant stage.

### 1.2.4 Rotational Positioning Mechanisms

Translational micropositioning mechanisms have drawn the attention of numerous researchers [19] because they are relatively easy to implement. Nevertheless, for many scenarios such as semiconductor manufacturing, microalignment devices, and optics devices [31], a micropositioning system which is capable of precision rotary positioning is required. Unfortunately, only limited previous work can be found in this category.

In the literature, compliant stages providing combined translational and rotational motions have been reported [32–34]. For example, Fig. 1.8 shows a planar three-revolute-revolute-revolute (3-RRR) flexure parallel mechanism, which can provide two translational motions in the  $xy$ -plane and one rotational motion around the  $z$ -axis. Spatial compliant mechanisms have also been reported to deliver coupled translations and rotations in three-dimensional space [35]. Additionally, precision stages with spherical motions have been developed [36]. This book involves the design and implementation of rotational compliant micropositioning stages which are capable of pure rotary motion. Such rotary stages have found extensive applications in precision engineering. Several rotational flexure stages have been proposed in previous work [37–40]. However, the majority of existing stages are only able to deliver a small rotary angle less than  $1^\circ$ . In practice, a rotational stage with a larger angle is demanded in many situations. How to achieve a large rotary range by using flexure-based compliant mechanisms is a major challenge.

A conventional compliant rotational stage is illustrated in Fig. 1.9. The rotational stage is guided by radial flexures with fixed-guided constraint [39, 41, 42], as shown in Fig. 1.10(a). The circle-like output platform can rotate around the center of the stage. However, its rotational range is limited due to the mechanism overconstraint and stress stiffening effect [43]. To enlarge the rotary angle, several rotational bearings have been presented [44–46] and some rotational stages driven by smart material-based actuators (e.g., piezoelectric actuator and shape memory alloy) have been devised [47]. For instance, a butterfly-shaped flexure pivot is reported [44], which exhibits the characteristics of small parasitic center translation and monolithic structure. More recently, a large-displacement compliant

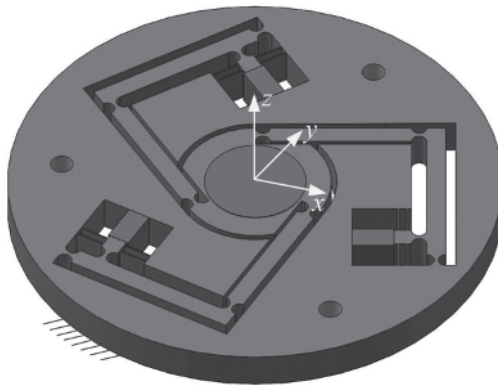


**Figure 1.8** Example of a flexure-based compliant 3-RRR parallel stage.

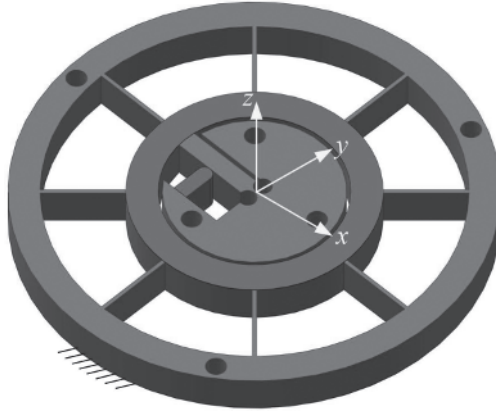


**Figure 1.9** Example of a flexure-based compliant rotational stage.

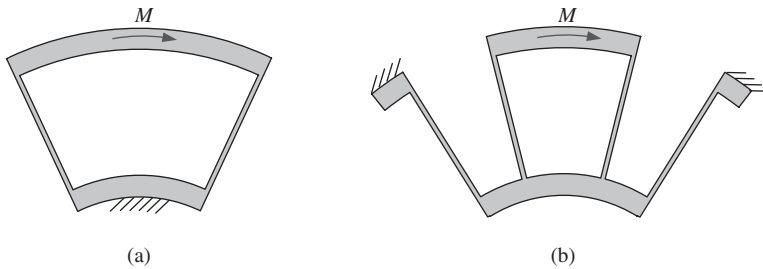


**Figure 1.10** (a) A radial flexure; (b) a compound radial flexure (CRF).

rotational hinge called Flex-16 has been proposed [46], which is able to rotate  $90^\circ$  without failure.

Alternatively, the basic module of radial flexure can be employed to construct compound radial flexures (CRFs) [48], as illustrated in Fig. 1.10(b). To achieve a large rotational range, the CRFs should be designed with larger length, smaller thickness, and larger outer radius. However, these physical parameters are restricted by the compactness constraint, manufacturing tolerance, and requirement on the minimum stiffness in practice. Thus, it is difficult to achieve a large rotational range while maintaining a compact stage size by using CRFs.

To cope with the above problem, the concept of multi-stage compound radial flexure (MCRF) [49] is employed in this book to devise a rotational stage with enlarged rotary angle as well as compact physical dimension. One kind of MCRF with two modules is shown in Fig. 1.11(a). Furthermore, to enhance the transverse stiffness in the radial direction (toward the rotation center), an improved MCRF is given in Fig. 1.11(b), which is constructed by connecting the two secondary stages together.

A survey on the recent development of large-stroke compliant micropositioning stages has been reported in the literature [50].

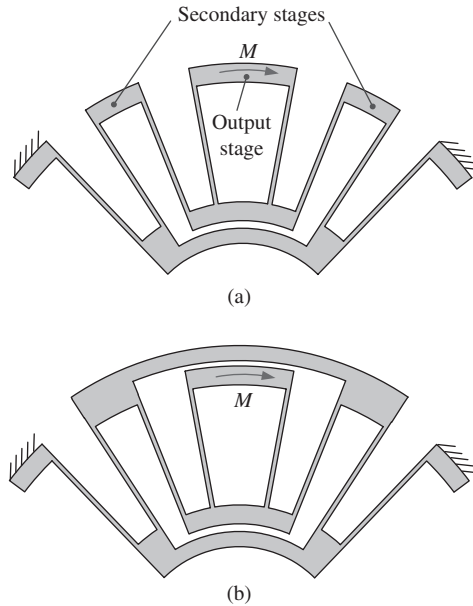


**Figure 1.11** (a) A multi-stage compound radial flexure (MCRF) with two modules; (b) an improved MCRF with enhanced stiffness in the radial direction.

### 1.2.5 Multi-Stroke Positioning Mechanisms

Multi-stroke micropositioning is highly desirable in scenarios where the merits of high positioning accuracy, long stroke motion, and high servo bandwidth are simultaneously required. Usually, a dual-servo system (DSS) is employed to deliver a coarse motion and a fine motion together. In applications such as scanning probe microscopy (SPM), a precision nanopositioning stage is used to implement an accurate and rapid raster scanning operation to get surface profiles of the scanned specimen [51, 52]. Nevertheless, only a small portion of the specimen can be put on the scanning table. For instance, an atomic force microscope (AFM) usually delivers a scanning range less than  $200\ \mu\text{m} \times 200\ \mu\text{m}$ . In order to acquire the surface topography of a large specimen (e.g.,  $10\ \text{mm} \times 10\ \text{mm}$ ), a nanopositioning stage with both a large workspace and a high bandwidth is required to fully cover the whole specimen surface and to quickly acquire the surface profile of interested scanning areas, as illustrated in Fig. 1.12. Thus, the DSS opens the way to cater for these demands. DSSs also have promising applications in biological micromanipulation [53] and microgripping [54].

Most of the existing DSSs are applied in hard-disk drives [55]. Recently, DSSs have been extended to micro-/nanopositioning applications. For example, a dual-stage nanopositioning system is developed in [56], where a coarse permanent magnet stepper motor stage and a fine piezoelectric stack actuator stage are stacked together. A coarse/fine dual-stage system is reported in [57] by using a voice coil motor to drive a fine stage and a permanent magnet linear synchronous motor to drive a coarse stage. Additionally, the design of a linear dual-stage actuation system is presented [8] by employing a voice coil motor and a piezoelectric stack actuator as the coarse and fine drivers, respectively. In the foregoing work, aerostatic bearings

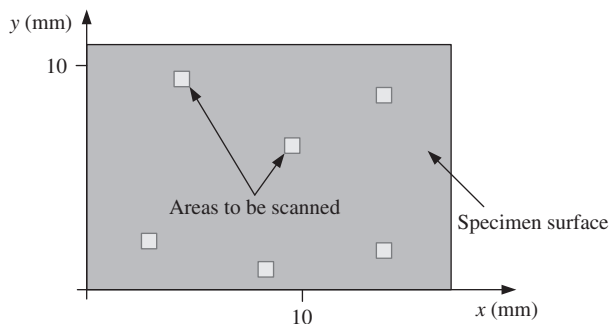


**Figure 1.12** Illustration of required scan area over the surface of a large specimen.

and maglev bearings are most adopted to guide the output motion of the stage. By contrast, flexure bearings are preferred due to their merits of no backlash, no friction, vacuum compatibility, easy manufacturing, and so on. Thus, flexures are employed in the recent development of dual-stage micro-/nanopositioning systems [58–60].

The major issue of a dual-servo stage arises from the interference behavior, which is caused by the interaction between the coarse and fine stages. In this book, the idea of mechanical decoupling design is introduced to minimize the interference behavior. In addition, one actuator conventionally only delivers a single stroke along with a specific resolution. It is challenging to devise a single-drive stage with multiple strokes as well as multiple resolutions. In this book, different conceptual designs of multi-stroke flexure-based micropositioning systems will be presented.

### 1.3 Actuation and Sensing

The micropositioning stage is usually called a nanopositioning stage if it can deliver a motion resolution at (sub-)nanometer level. Because the compliant mechanism can deliver a smooth and repeatable motion, the generation of ultrahigh-level resolution for flexure-based micropositioning systems is dependent on the selection of actuators and sensors.

Piezoelectric stack actuators (PSAs) are widely applied in micro-/nanopositioning stages. However, PSAs typically deliver a short stroke up to 0.1% of their length [61]. Although various lever transmission mechanisms can be employed to amplify the output displacement [62, 63], it is practically difficult to realize a positioning over 10 mm. In order to achieve a large motion range, the ball-screw drives are mostly employed [64]. Such actuation produces a large motion range yet introduces nonlinearity in terms of the friction effect, which may deteriorate the positioning accuracy. In addition, the stick–slip actuators have been reported to provide unlimited strokes in theory [65]. However, the stick–slip motion is usually achieved by resorting to the friction force, which may induce mechanical wear and block the achievement of continuous and accurate motion. Hence, some friction-free drives have been employed, such as magnetic levitation motors [66], electromagnetic actuators [67], and voice coil motors (VCMs) [68, 49].

These types of motors are lubrication free and vacuum compatible, hence also fulfilling applications in ultraclean environments. Without loss of generality, the VCMs are employed

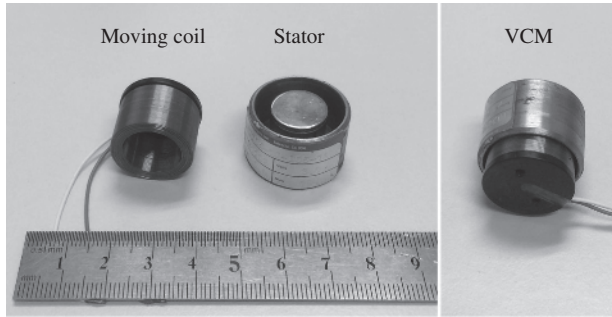


**Figure 1.13** A linear voice coil motor (VCM).

to drive the large-range micropositioning stages. The VCM is a linear or rotary actuator, which consists of a permanent magnetic stator and a moving cylinder encompassed by a coil of copper wire. A photograph of a linear VCM (model: NCC04-10-005-1A, from H2W Techniques, Inc.) and its components is shown in Fig. 1.13, which can provide a linear stroke of 10.2 mm. The VCM works based on Lorentz force law. That is, a current-carrying wire in a magnetic field creates a force which is perpendicular to the directions of the current and the magnetic field. Recent applications of VCMs in high-precision positioning stages are reviewed in [69]. In this book, both linear and rotary VCMs are used to actuate the translational and rotational micropositioning systems.

Concerning the sensing issue, the output displacement of a micropositioning device can be measured by various displacement sensors based on different sensing principles [70]. In the literature, optical sensors, capacitive sensors, strain sensors, and inductance sensors have been employed in micropositioning systems. In this book, the laser displacement sensors, capacitive sensors, and strain-gauge sensors are selected as examples in the prototype implementations. To achieve nanometer-level resolution in a large positioning range for the large-range micropositioning systems, laser interferometers can be adopted.

In this book, the micropositioning systems are designed to provide the specified large-range translational or rotational motion in determinate directions. Depending on the materials, the micropositioning stages can be fabricated by resorting to wire-electrical discharge machining (EDM), laser cutting, and water-jet cutting processes. As an alternative type of compliant mechanism, soft mechanisms have recently been developed to deliver the large-range motion in an arbitrary direction [71]. Such a robotic mechanism is usually designed based on soft and deformable materials and driven by pneumatic, hydraulic, and smart material-based actuators, etc. Concerning manufacture, the soft mechanisms are usually fabricated by means of rapid prototyping (RP), 3-D printing, and so on.

## 1.4 Control Issues

Once the micropositioning stage is fabricated, the achievement of precision positioning is dependent on the control technique. Due to the low damping of the flexure-based system, a number of vibration modes exist and a high-order model is commonly identified for the system plant, which may result in a high-order controller as a consequence. From the implementation

point of view, a linear model of lower order (e.g., second order) is more desirable for practical realization of the control algorithm. However, the adoption of a low-order model means that the residual modes are not considered. Challenges exist in control design because the neglect of residual modes may cause control spillover and observation spillover [72]. Spillover is undesirable as it may cause instability and performance degradation of the system [73]. In addition, to facilitate the control design, model nonlinearity including the hysteresis effect is usually considered as a lumped disturbance to the nominal plant model. The suppression of the disturbance requires a robust control approach.

To account for these problems, various control techniques have been developed to maintain the robustness of the system in the presence of model uncertainties and disturbances. The block diagram of a typical feedback control is shown in Fig. 1.14. Nowadays, the most popular control approach in various industrial domains is proportional-integral-derivative (PID) control [74]. One reason for this is that, as a model-free control scheme, PID is easy to maintain in practice. However, PID control exhibits weak robustness against system uncertainties and external disturbances. Hence, it cannot always produce satisfactory control results for some applications where the plants are accompanied by nonlinearities and disturbances. To achieve better performance for a micropositioning system, advanced control schemes have been employed, such as the gain scheduling control [75], loop shaping technique [76],  $H_\infty$  robust control [77], adaptive control [78], model-reference control [79], repetitive control [80], iterative learning control [81], fuzzy logic control [82], and neuro-fuzzy control [83], to name just a few.

Moreover, sliding mode control (SMC) has been demonstrated as a simple yet efficient nonlinear robust control approach to tolerate model uncertainty and disturbance. The essence of SMC is to drive the system state trajectory onto a specified sliding manifold and then keep it moving along the surface. Once the sliding surface is reached, the controlled system is robust against certain variation of the model and external disturbances. In recent years, a variety of SMC strategies have been developed for precision motion systems [84]. Furthermore, discrete-time sliding mode control (DSMC) is more feasible for implementation on sampled-data systems [85]. A DSMC scheme can be developed based on the system state or system output [86, 87]. In a typical micropositioning system, only the position information is supplied by the displacement sensors. In order to realize the DSMC scheme, a state observer is usually needed if the full state information is required [88]. Some recent DSMC strategies have been developed to eliminate the use of a state observer [89].

Additionally, as a robust control strategy, model predictive control (MPC) is well-known for its ability to solve the problems with constraints, time delays, and disturbances by offering an optimal control action [90]. The essence of the MPC scheme is to obtain the current

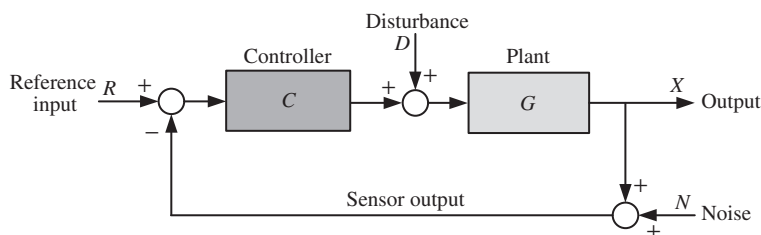


**Figure 1.14** Block diagram of feedback control of a micropositioning system.

control action by optimizing the predictions of plant behavior over a finite sequence of future control inputs. At each sampling time instant, the MPC controller generates an optimal control sequence by solving an optimization problem and uses the first element of the sequence as the control action for the system plant. Recently, MPC schemes have been widely employed in the domain of precision motion control [87, 91].

Regarding micro-/nanopositioning systems driven by piezoelectric actuators, advanced control methodologies have been presented in a recent monograph [92]. In this book, typical control algorithms including PID, DSMC, and MPC are implemented to demonstrate the performance of the developed micropositioning systems.

## 1.5 Book Outline

According to the different implementations of the micropositioning systems, the remaining ten chapters of the book are divided into four parts. Part I presents the design and implementation of large-range translational micropositioning systems. Part II develops the design and development of multi-stroke translational micropositioning systems. Part III proposes the design and realization of large-range rotational micropositioning systems. As typical applications of the devised translational and rotational micropositioning systems, Part IV reports on the design and development of innovative large-range compliant grippers.

All the chapters involve both simulation and experimental verification studies. Moreover, further research directions following each chapter are proposed as potential future work. The presented design ideas can easily be extended to the design of various MEMS devices. Even though planar motion is mostly concerned in this book, the presented design methodologies can be expanded to the design of spatial compliant mechanisms to achieve three-dimensional large-range motion for pertinent applications.

## References

- [1] Howell, L.L. (2001) *Compliant Mechanisms*, Wiley, New York.
- [2] Lobontiu, N. (2002) *Compliant Mechanisms: Design of Flexure Hinges*, CRC Press, Boca Raton, FL.
- [3] Sinno, A., Ruaux, P., Chassagne, L., Topcu, S., Alayli, Y., Lerondel, G., et al. (2007) Enlarged atomic force microscopy scanning scope: Novel sample-holder device with millimeter range. *Rev. Sci. Instrum.*, **78** (9), 095 107.
- [4] Lee, D.J., Kim, K., Lee, K.N., Choi, H.G., Park, N.C., Park, Y.P. et al. (2010) Robust design of a novel three-axis fine stage for precision positioning in lithography. *Proc. Inst. Mech. Eng. Part C-J. Mech. Eng. Sci.*, **224** (4), 877–888.
- [5] Gauthier, M. and Piat, E. (2006) Control of a particular micro-macro positioning system applied to cell micro-manipulation. *IEEE Trans. Automat. Sci. Eng.*, **3** (3), 264–271.
- [6] Huang, H.B., Sun, D., Mills, J.K., and Cheng, S.H. (2009) Robotic cell injection system with position and force control: Toward automatic batch biomanipulation. *IEEE Trans. Robot.*, **25** (3), 727–737.
- [7] Zhang, Y.L., Zhang, Y., Ru, C., Chen, B.K., and Sun, Y. (2013) A load-lock-compatible nanomanipulation system for scanning electron microscope. *IEEE/ASME Trans. Mechatron.*, **18** (1), 230–237.
- [8] Dong, W., Tang, J., and ElDeeb, Y. (2009) Design of a linear-motion dual-stage actuation system for precision control. *Smart Mater. Struc.*, **18**, 095 035–1–095 035–11.
- [9] Chen, M.Y., Wang, C.C., and Fu, L.C. (2001) Adaptive sliding mode controller design of a dual-axis maglev positioning system, in *Proc. American Control Conf.*, Arlington, VA, pp. 3731–3736.
- [10] Hegde, S. and Ananthasuresh, G.K. (2012) A spring-mass-lever model, stiffness and inertia maps for single-input, single-output compliant mechanisms. *Mech. Mach. Theory*, **58**, 101–119.

- [11] Howell, L.L. and Midha, A. (1995) Parametric deflection approximations for end-loaded, large-deflection beams in compliant mechanisms. *J. Mech. Des.*, **117** (1), 156–165.
- [12] Bernardoni, P., Bidaud, P., Bidard, C., and Gosselin, F. (2004) A new compliant mechanism design methodology based on flexible building blocks, in *Proc. SPIE*, vol. 5383, San Diego, CA, vol. 5383, pp. 244–254.
- [13] Wang, M.Y., Wang, X., and Guo, D. (2003) A level set method for structural topology optimization. *Comput. Meth. Appl. Mech. Eng.*, **192** (1), 227–246.
- [14] Hopkins, J.B. and Culpepper, M.L. (2010) Synthesis of multi-degree of freedom, parallel flexure system concepts via freedom and constraint topology (FACT)-part I: Principles. *Precis. Eng.*, **34** (2), 259–270.
- [15] Yong, Y.K., Lu, T.F., and Handley, D.C. (2008) Review of circular flexure hinge design equations and derivation of empirical formulations. *Precis. Eng.*, **32** (2), 63–70.
- [16] Smith, S.T. (2000) *Flexures: Elements of Elastic Mechanisms*, Gordon and Breach, New York.
- [17] Trease, B.P., Moon, Y.M., and Kota, S. (2004) Design of large-displacement compliant joints. *J. Mech. Des.*, **127** (4), 788–798.
- [18] Krijnen, B., Swinkels, K.R., Brouwer, D.M., Abelmann, L., and Herder, J.L. (2015) A large-stroke 3DOF stage with integrated feedback in MEMS. *J. Microelectromech. Syst.*, **24** (6), 1720–1729.
- [19] Xu, Q. (2012) New flexure parallel-kinematic micropositioning system with large workspace. *IEEE Trans. Robot.*, **28** (2), 478–491.
- [20] Fung, R.F., Hsu, Y.L., and Huang, M.S. (2009) System identification of a dual-stage XY precision positioning table. *Precis. Eng.*, **33** (1), 71–80.
- [21] Kenton, B.J. and Leang, K.K. (2012) Design and control of a three-axis serial-kinematic high-bandwidth nanopositioner. *IEEE/ASME Trans. Mechatron.*, **17** (2), 356–369.
- [22] Wadikhaye, S., Yong, Y.K., and Moheimani, S.O.R. (2012) Design of a compact serial-kinematic scanner for high-speed atomic force microscopy: An analytical approach. *Micro Nano Lett.*, **7** (4), 309–313.
- [23] Yong, Y.K. and Lu, T.F. (2009) Kinetostatic modeling of 3-RRR compliant micro-motion stages with flexure hinges. *Mech. Mach. Theory*, **44** (6), 1156–1175.
- [24] Ramadan, A.A., Takubo, T., Mae, Y., Oohara, K., and Arai, T. (2009) Developmental process of a chopstick-like hybrid-structure two-fingered micromanipulator hand for 3-D manipulation of microscopic objects. *IEEE Trans. Ind. Electron.*, **56** (4), 1121–1135.
- [25] Merlet, J.P. (2006) *Parallel Robots*, Springer, Berlin.
- [26] Kang, D., Kim, K., Kim, D., Shim, J., Gweon, D.G., and Jeong, J. (2009) Optimal design of high precision XY-scanner with nanometer-level resolution and millimeter-level working range. *Mechatronics*, **19** (4), 562–570.
- [27] Chen, M.Y., Huang, H.H., and Hung, S.K. (2010) A new design of a submicropositioner utilizing electromagnetic actuators and flexure mechanism. *IEEE Trans. Ind. Electron.*, **57** (1), 96–106.
- [28] Awtar, S. and Parmar, G. (2010) Design of a large range XY nanopositioning system, in *Proc. ASME 2010 Int. Design Engineering Technical Conf.*, Montreal, Canada, pp. 387–399.
- [29] Hao, G. and Kong, X. (2012) A novel large-range XY compliant parallel manipulator with enhanced out-of-plane stiffness. *J. Mech. Des.*, **134** (6), 061009.
- [30] Xu, Q. and Li, Y. (2006) Stiffness modeling for an orthogonal 3-PUU compliant parallel micromanipulator, in *Proc. IEEE Int. Conf. on Mechatronics and Automation*, Luoyang, Henan, China, pp. 124–129.
- [31] Chong, J., He, S., and Ben Mrad, R. (2012) Development of a vector display system based on a surface-micromachined micromirror. *IEEE Trans. Ind. Electron.*, **59** (12), 4863–4870.
- [32] Wang, H. and Zhang, X. (2008) Input coupling analysis and optimal design of a 3-DOF compliant micro-positioning stage. *Mech. Mach. Theory*, **43** (4), 400–410.
- [33] Hwang, D., Byun, J., Jeong, J., and Lee, M.G. (2011) Robust design and performance verification of an in-plane XY $\theta$  micropositioning stage. *IEEE Trans. Nanotechnol.*, **10** (6), 1412–1423.
- [34] Qin, Y., Shirinzadeh, B., Zhang, D., and Tian, Y. (2013) Design and kinematics modeling of a novel 3-DOF monolithic manipulator featuring improved Scott–Russell mechanisms. *J. Mech. Des.*, **135** (10), 101004.
- [35] Yang, G., Teo, T.J., Chen, I.M., and Lin, W. (2011) Analysis and design of a 3-DOF flexure-based zero-torsion parallel manipulator for nano-alignment applications, in *Proc. IEEE Int. Conf. on Robotics and Automation*, Shanghai, China, pp. 2751–2756.
- [36] Tan, K.K., Huang, S., Liang, W., Mamun, A.A., Koh, E.K., and Zhou, H. (2012) Development of a spherical air bearing positioning system. *IEEE Trans. Ind. Electron.*, **59** (9), 3501–3509.
- [37] Cannon, J.R. and Howell, L.L. (2005) A compliant contact-aided revolute joint. *Mech. Mach. Theory*, **40** (11), 1273–1293.

- [38] Wang, Y.C. and Chang, S.H. (2006) Design and performance of a piezoelectric actuated precise rotary positioner. *Rev. Sci. Instrum.*, **77** (10), 105–101.
- [39] Kim, K., Ahn, D., and Gweon, D. (2012) Optimal design of a 1-rotational DOF flexure joint for a 3-DOF H-type stage. *Mechatronics*, **22** (1), 24–32.
- [40] Teo, T.J., Yang, G., and Chen, I.M. (2014) A large deflection and high payload flexure-based parallel manipulator for UV nanoimprint lithography: Part I. Modeling and analyses. *Precis. Eng.*, **38** (4), 861–871.
- [41] Luo, H.P., Zhang, B., and Zhou, Z.X. (2008) A rotary flexural bearing for micromanufacturing. *CIRP Ann.-Manuf. Techn.*, **57**, 179–182.
- [42] Bi, S., Zhao, S., and Zhu, X. (2010) Dimensionless design graphs for three types of annulus-shaped flexure hinges. *Precis. Eng.*, **34** (3), 659–666.
- [43] Choi, Y.J., Sreenivasan, S.V., and Choi, B.J. (2008) Kinematic design of large displacement precision XY positioning stage by using cross strip flexure joints and over-constrained mechanism. *Mech. Mach. Theory*, **43** (6), 724–737.
- [44] Henein, S., Spanoudakis, P., Droz, S., Myklebust, L.I., and Onillon, E. (2003) Flexure pivot for aerospace mechanisms, in *Proc. 10th European Space Mechanisms and Tribology Symp.*, San Sebastian, Spain, pp. 1–4.
- [45] Pei, X., Yu, J., Zong, G., Bi, S., and Su, H. (2009) The modeling of cartwheel flexural hinges. *Mech. Mach. Theory*, **44** (10), 1900–1909.
- [46] Fowler, R.M., Maselli, A., Pluimers, P., Magleby, S.P., and Howell, L.L. (2014) Flex-16: A large-displacement monolithic compliant rotational hinge. *Mech. Mach. Theory*, **82**, 203–217.
- [47] Li, J., Zhao, H., Qu, H., Cui, T., Fu, L., Huang, H., et al. (2013) A piezoelectric-driven rotary actuator by means of inchworm motion. *Sens. Actuator A-Phys.*, **194**, 269–276.
- [48] Valois, M. (2012), Rotary flexure bearing. US 2012/0034027 A1.
- [49] Xu, Q. (2013) Design and implementation of a novel rotary micropositioning system driven by linear voice coil motor. *Rev. Sci. Instrum.*, **84** (5), 055 001.
- [50] Wan, S. and Xu, Q. (2014) A survey on recent development of large-stroke compliant micropositioning stage. *Int. J. Robot. Automat. Technol.*, **1** (1), 19–35.
- [51] Mokaberi, B. and Requicha, A.A.G. (2008) Compensation of scanner creep and hysteresis for AFM nanomanipulation. *IEEE Trans. Automat. Sci. Eng.*, **5** (2), 197–206.
- [52] Leang, K.K., Zou, Q., and Devasia, S. (2009) Feedforward control of piezoactuators in atomic force microscope systems: Inversion-based compensation for dynamics and hysteresis. *IEEE Control Syst. Mag.*, **29** (1), 70–82.
- [53] Gauthier, M. and Piat, E. (2006) Control of a particular micro-macro positioning system applied to cell micro-manipulation. *IEEE Trans. Automat. Sci. Eng.*, **3** (3), 264–271.
- [54] Rakotondrabe, M. and Ivan, I.A. (2011) Development and force/position control of a new hybrid thermo-piezoelectric microgripper dedicated to micromanipulation tasks. *IEEE Trans. Automat. Sci. Eng.*, **8** (4), 824–834.
- [55] Al Mamun, A., Mareels, I., Lee, T.H., and Tay, A. (2003) Dual-stage actuator control in hard disk drive – a review, in *Proc. 29th Annual IEEE Industrial Electronics Society Conf.*, pp. 2132–2137.
- [56] Michellod, Y., Mullhaupt, P., and Gillet, D. (2006) Strategy for the control of a dual-stage nano-positioning system with a single metrology, in *Proc. IEEE Conf. on Robotics, Automation and Mechatronics*, pp. 1–8.
- [57] Song, Y., Wang, J., Yang, K., Yin, W., and Zhu, Y. (2010) A dual-stage control system for high-speed, ultra-precise linear motion. *Int. J. Adv. Manuf. Technol.*, **48**, 633–643.
- [58] Dong, W., Sun, L.N., and Du, Z.J. (2007) Design of a precision compliant parallel positioner driven by dual piezoelectric actuators. *Sens. Actuator A-Phys.*, **135** (1), 250–256.
- [59] Xu, Q. (2012) Design and development of a flexure-based dual-stage nanopositioning system with minimum interference behavior. *IEEE Trans. Automat. Sci. Eng.*, **9** (3), 554–563.
- [60] Tuma, T., Haerberle, W., Rothuizen, H., Lygeros, J., Pantazi, A., and Sebastian, A. (2014) Dual-stage nanopositioning for high-speed scanning probe microscopy. *IEEE/ASME Trans. Mechatron.*, **19** (3), 1035–1045.
- [61] Yao, Q., Dong, J., and Ferreira, P.M. (2007) Design, analysis, fabrication and testing of a parallel-kinematic micropositioning XY stage. *Int. J. Mach. Tools Manuf.*, **47** (6), 946–961.
- [62] Kim, J.J., Choi, Y.M., Ahn, D., Hwang, B., Gweon, D.G., and Jeong, J. (2012) A millimeter-range flexure-based nano-positioning stage using a self-guided displacement amplification mechanism. *Mech. Mach. Theory*, **50**, 109–120.
- [63] Xu, Q. and Li, Y. (2011) Analytical modeling, optimization and testing of a compound bridge-type compliant displacement amplifier. *Mech. Mach. Theory*, **46** (2), 183–200.
- [64] Otsuka, J., Ichikawa, S., Masuda, T., and Suzuki, K. (2005) Development of a small ultraprecision positioning device with 5 nm resolution. *Meas. Sci. Technol.*, **16** (11), 2186.

- [65] Breguet, J.M. and Clavel, R. (1998) Stick and slip actuators: Design, control, performances and applications, in *Proc. Int. Symp. on Micromechatronics and Human Science*, pp. 89–95.
- [66] Verma, S., Kim, W.J., and Gu, J. (2004) Six-axis nanopositioning device with precision magnetic levitation technology. *IEEE/ASME Trans. Mechatron.*, **9** (2), 384–391.
- [67] Kim, D.H., Lee, M.G., Kim, B., and Sun, Y. (2005) A superelastic alloy microgripper with embedded electromagnetic actuators and piezoelectric force sensors: A numerical and experimental study. *Smart Mater. Struct.*, **14** (6), 1265–1272.
- [68] Rakuff, S. and Cuttinob, J.F. (2009) Design and testing of a long-range, precision fast tool servo system for diamond turning. *Precis. Eng.*, **33** (1), 18–25.
- [69] Shan, G., Li, Y., Zhang, L., Wang, Z., Zhang, Y., and Qian, J. (2015) Application of voice coil motors in high-precision positioning stages with large travel ranges. *Rev. Sci. Instrum.*, **86** (10), 101 501.
- [70] Ouyang, P.R., Tjioptrodjo, R.C., Zhang, W.J., and Yang, G.S. (2008) Micro-motion devices technology: The state of arts review. *Int. J. Adv. Manuf. Technol.*, **38** (5&6), 463–478.
- [71] Rus, D. and Tolley, M.T. (2015) Design, fabrication and control of soft robots. *Nature*, **521** (7553), 467–475.
- [72] Pai, M.C. and Sinha, A. (2000) Sliding mode control of vibration in a flexible structure via estimated states and  $H_\infty/\mu$  techniques, in *Proc. American Control Conf.*, Baltimore, MD, pp. 1118–1123.
- [73] Wang, D.A. and Huang, Y.M. (2003) Application of discrete-time variable structure control in the vibration reduction of a flexible structure. *J. Sound Vibr.*, **261** (3), 483–501.
- [74] Jaensch, M. and Lamperth, M.U. (2007) Investigations into the stability of a PID-controlled micropositioning and vibration attenuation system. *Smart Mater. Struct.*, **16** (4), 1066–1075.
- [75] Lee, S.Q., Kim, Y., and Gweon, D.G. (2000) Continuous gain scheduling control for a micro-positioning system: Simple, robust and no overshoot response. *Control Eng. Pract.*, **8** (2), 133–138.
- [76] Youm, W., Jung, J., Lee, S., and Park, K. (2008) Control of voice coil motor nanoscanners for an atomic force microscopy system using a loop shaping technique. *Rev. Sci. Instrum.*, **79** (1), 013 707.
- [77] Dong, J., Salapaka, S.M., and Ferreira, P.M. (2008) Robust control of a parallel-kinematic nanopositioner. *J. Dyn. Sys., Meas., Control*, **130** (4), 041 007–1–041 007–15.
- [78] Tan, X. and Baras, J.S. (2005) Adaptive identification and control of hysteresis in smart materials. *IEEE Trans. Automatic Control*, **50** (6), 827–839.
- [79] Xu, Q. and Jia, M. (2014) Model reference adaptive control with perturbation estimation for a micropositioning system. *IEEE Trans. Contr. Syst. Technol.*, **22** (1), 352–359.
- [80] Li, Y. and Xu, Q. (2012) Design and robust repetitive control of a new parallel-kinematic XY piezostage for micro/nanomanipulation. *IEEE/ASME Trans. Mechatron.*, **17** (6), 1120–1132.
- [81] Wu, Y. and Zou, Q. (2007) Iterative control approach to compensate for both the hysteresis and the dynamics effects of piezo actuators. *IEEE Trans. Contr. Syst. Technol.*, **15** (5), 936–944.
- [82] Chi, Z., Jia, M., and Xu, Q. (2014) Fuzzy PID feedback control of piezoelectric actuator with feedforward compensation. *Math. Probl. Eng.*, **2014**. Article ID 107184, doi: 10.1155/2014/107184.
- [83] Lin, L.C., Sheu, J.W., and Tsay, J.H. (2001) Modeling and hierarchical neuro-fuzzy control for flexure-based micropositioning systems. *J. Intell. Robot. Syst.*, **32** (4), 411–435.
- [84] Yu, X. and Kaynak, O. (2009) Sliding mode control with soft computing: A survey. *IEEE Trans. Ind. Electron.*, **56** (9), 3275–3285.
- [85] Gao, W., Wang, Y., and Homaifa, A. (1995) Discrete-time variable structure control systems. *IEEE Trans. Ind. Electron.*, **42** (2), 117–122.
- [86] Xu, J.X. and Abidi, K. (2008) Discrete-time output integral sliding-mode control for a piezomotor-driven linear motion stage. *IEEE Trans. Ind. Electron.*, **55** (11), 3917–3926.
- [87] Xu, Q. and Li, Y. (2012) Model predictive discrete-time sliding mode control of a nanopositioning piezostage without modeling hysteresis. *IEEE Trans. Contr. Syst. Technol.*, **20** (4), 983–994.
- [88] Ghafarirad, H., Rezaei, S.M., Abdullah, A., Zareinejad, M., and Saadat, M. (2011) Observer-based sliding mode control with adaptive perturbation estimation for micropositioning actuators. *Precis. Eng.*, **35** (2), 271–281.
- [89] Xu, Q. (2014) Digital sliding-mode control of piezoelectric micropositioning system based on input–output model. *IEEE Trans. Ind. Electron.*, **61** (10), 5517–5526.
- [90] Morari, M. and Lee, J.H. (1999) Model predictive control: Past, present and future. *Comput. Chem. Eng.*, **23** (4 & 5), 667–682.
- [91] Xu, Q. (2015) Digital sliding mode prediction control of piezoelectric micro/nanopositioning system. *IEEE Trans. Contr. Syst. Technol.*, **23** (1), 297–304.
- [92] Xu, Q. and Tan, K.K. (2015) *Advanced Control of Piezoelectric Micro-/Nano-Positioning Systems*, Springer, Berlin.

